Acceleration of Convergence to a Periodic Steady State in Turbomachinery Flows

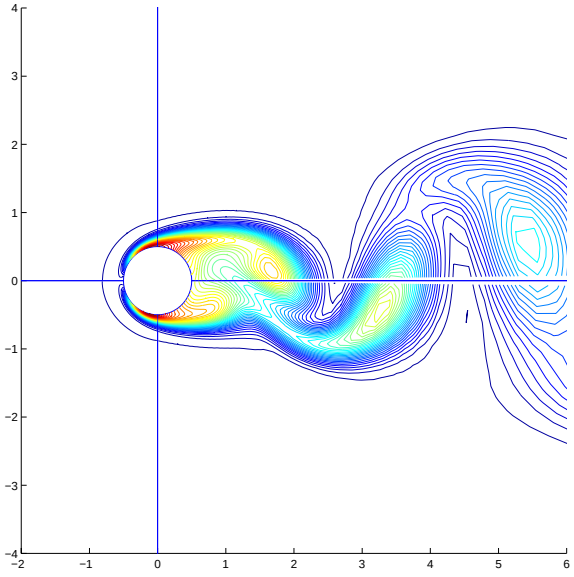

Matthew McMullen and Antony Jameson
and Juan J. Alonso
Dept. of Aeronautics & Astronautics
Stanford University

39th AIAA Aerospace Sciences Meeting & Exhibit
Reno, NV
January 8-11, 2000

Acknowledgments

- Department of Energy - Accelerated Strategic Computing Initiative (ASCI)

- Kenneth C. Hall - Associate Professor in the Mechanical Engineering and Materials Science Department, Duke University

Outline

- Motivation
- Governing Equations
- Boundary Conditions
- Solution Method
- Results
- Conclusions
- Future Work

Motivation

- The goal of ASCI is to calculate the unsteady flow of an aircraft gas turbine engine. This includes component simulations of the compressor, combustor, and turbine.

- TFLO is the ASCI compressor/turbine solver and is based on a dual time stepping technique.

- Dual time stepping algorithms implement a system of nested loops. Each physical time step is an iteration in the outer loop. The inner loop solves the discretization of the time derivative and implicit residual terms.

Motivation (cont.)

- Typically one restricts the number of inner iterations to the order of 30-80. Each inner iteration is a complete V-cycle with pseudo-local time stepping, and implicit residual averaging.

- In practice it has been found that on the order of 24-36 implicit time steps are sufficient to resolve the features of one period in the oscillation of the flow.

- At a minimum, capturing one period requires 1000 inner iterations.

Motivation (cont.)

Component	% Wheel	Total CPU Hours
Turbine	16	2.0 million
Compressor	16	5.4 million

- The job size typically varies between 500-1,000 processors. Queues limit the job execution to approximately 8 hours per day.

- ASCI has access to a variety of DOE machines. Different processor/machine combinations effect the overall execution duration, but estimates for job length are now provided in months.

Motivation (cont)

- For more information on ASCI research see:

Time	Title	Authors
Tuesday 4:30 PM	Unsteady Flow Investigation in Axial Turbines Using the Massively Parallel Flow Solver TFLO	Yao, Davis, Jameson, Alonso
Wednesday 2:00 PM	A Multi-Code-Coupling Interface for Combustor/Turbomachinery Simulations	Shankaran Alonso, Davis Liou, Liu

Motivation (cont.)

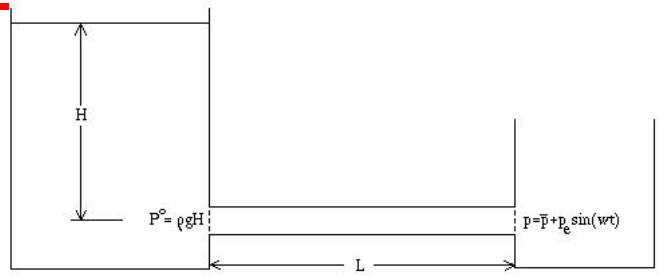

- A simplified analog of component simulations is one-dimensional unsteady channel flow. Merkle and Athavale (1987) have derived an analytic solution based on linearized perturbations. For an initially steady flow the velocity perturbations has the following solution.

$$\acute{u} = -\frac{\acute{p}_e}{\rho\bar{u}}\left(\frac{1}{1+\Omega^2}\right)\left[sin(wt) - \Omega cos(wt) + \Omega e^{-\frac{\bar{u}t}{L}}\right]$$

$$\Omega = \frac{wL}{\bar{u}}$$

Motivation (cont.)

- The rate of decay of the initial transients is proportional to $\frac{\bar{u}}{L}$ which represents the frequency at which information can travel the length of the duct.

- As the mean velocity decreases or the overall length increases the decay of the original transients is affected exponentially.

- The efficiency of any time accurate solver is now a function of the decay rate of the initial transients.

- In compressor/turbine calculations the blades and stators reflect unsteady perturbations. The transmission of these perturbations, back and forth, through 9 blade rows (current ASCI turbine simulation) effectively increases the overall length scale of the computation.

Motivation (cont.)

- Harmonic balance techniques transform the unsteady equations in the physical domain into a steady problem in the frequency domain.

- The process of finding a steady solution to the transformed equations does not waste time resolving the initial transients and their decay.

- To further decrease the computational cost of the frequency domain solver, users can limit the number of temporal modes with the understanding of the end requirements of the data.

Governing Equations

- Navier-Stokes Equations in integral form

$$\int \frac{\partial W}{\partial t} dV + \oint \vec{F} \cdot \vec{N} ds = 0$$

$$W = \begin{bmatrix} \rho \\ \rho u \\ \rho v \\ \rho E \end{bmatrix}$$

$$\vec{F}_i = f = \begin{bmatrix} \rho u \\ \rho u^2 + p - \sigma_{xx} \\ \rho uv - \sigma_{xy} \\ \rho uH - u\sigma_{xx} - v\sigma_{xy} + q_x \end{bmatrix} \qquad \vec{F}_j = g = \begin{bmatrix} \rho v \\ \rho uv - \sigma_{xy} \\ \rho v^2 + p - \sigma_{yy} \\ \rho vH - u\sigma_{xy} - v\sigma_{yy} + \end{bmatrix}$$

Governing Equations (cont.)

- Closure is provided by the following equations:

$$p = (\gamma - 1)\rho[e - \frac{1}{2}(u^2 + v^2)]$$

$$\sigma_{xx} = 2\mu u_x - \frac{2}{3}\mu(u_x + v_y)$$

$$\sigma_{yy} = 2\mu v_y - \frac{2}{3}\mu(u_x + v_y)$$

$$\sigma_{xy} = \sigma_{yx} = \mu(u_y + v_x)$$

$$q_x = \kappa\frac{\partial T}{\partial x} = -\frac{\gamma}{\gamma - 1}\frac{\mu}{Pr}\frac{\partial \frac{p}{\rho}}{\partial x}$$

$$q_y = \kappa\frac{\partial T}{\partial y} = -\frac{\gamma}{\gamma - 1}\frac{\mu}{Pr}\frac{\partial \frac{p}{\rho}}{\partial y}$$

Governing Equations (cont.)

- Approximating the volumetric integral for a given cell with volume V

$$\int \frac{\partial W}{\partial t} dV \approx V \frac{\partial W}{\partial t}$$

- Using the steady state residual variable $R(W)$ we can approximate the boundary integral as a sum of fluxes over a finite number of cell walls

$$\oint \vec{F} \cdot \vec{N} ds \approx R(W) = \sum_{j=1}^{n} \vec{F}_j \cdot \vec{S}_j$$

Governing Equations (cont.)

- Using the notation introduced above the integral form of the Navier-Stokes equation simplifies to

$$V\frac{\partial W}{\partial t} + R(W) = 0$$

- Expanding both W and $R(W)$ with a Fourier series in time

$$W = \sum_{k=-\frac{N}{2}}^{\frac{N}{2}-1} \hat{W}_k e^{ikt} \qquad R(W) = \sum_{k=-\frac{N}{2}}^{\frac{N}{2}-1} \hat{R}_k e^{ikt}$$

Governing Equations (cont.)

- It follows that a periodic steady-state equation can be written for each independent wave number. We add in a pseudo-time derivative and numerically integrate the equations.

$$V\frac{d\hat{W}_k}{d\tau} + ikV\hat{W}_k + \hat{R}_k = 0$$

- Each iterative step in the solution process requires the following data flow.

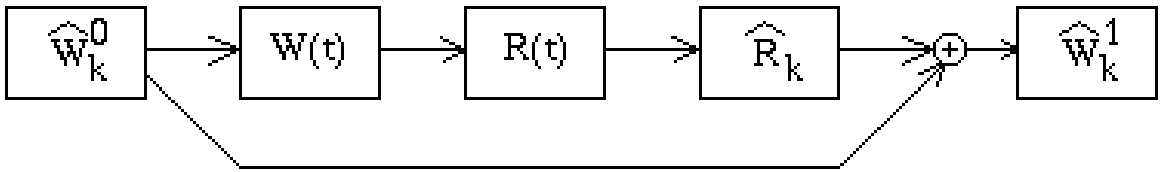

Boundary Conditions

- The solution at every interior grid point is expressed as Fourier coefficient. The boundary condition implementation takes advantage of the fact that we know the time average and oscillating components of the solution.

  Riemann invariants applied to the mean flow solution.
  Giles boundary conditions applied to all higher harmonics.

- Radiation boundary conditions zeroize the incoming characteristics. Inlet/exit boundary conditions for the channel specify the incoming characteristics. Implicit formulations for these boundary conditions were developed that improved the model's convergence and simplifying boundary condition implementation within the multigrid environment.

Solution Method

- Since we are dealing with solving a steady system of equations, we apply established methods to accelerate the convergence.

  Multi-stage RK scheme with local time stepping
  Implicit residual averaging
  Multigrid V-Cycle

- In addition, we are dealing with real functions where the Fourier coefficients for the positive wavenumbers are equal to the complex conjugates of the Fourier coefficients for the negative wavenumbers. This eliminates computation required to integrate the negative wave numbers forward in pseudo-time.

Solution Method (cont.)

- To begin a stability analysis we assume a linearization using only one space dimension.

$$\frac{d\hat{W}_k}{d\tau} + ik\hat{W}_k + A\frac{\partial \hat{W}_k}{\partial x} = 0$$

- Using a von Neumann test we expand the solution using a single spatial Fourier mode.

$$\frac{d\check{W}}{d\tau} + ik\check{W} + \frac{M}{\Delta x}\check{W} = 0$$

Solution Method (cont.)

- M is the spectral matrix corresponding to the spatial discretization. For example with central differences

$$M = Ai \sin(\omega \Delta x)$$

- Splitting the maximum eigenvalue of M into a real $\bar{\lambda}_r$ and imaginary $\bar{\lambda}_i$ part, we arrive at a simplified equation (for the characteristic variable $\dot{W}$) containing the additional terms introduced by the harmonic balance technique.

$$\frac{d\dot{W}}{d\tau} = -\left[\frac{\bar{\lambda}_r}{\Delta x} + \left(\frac{\bar{\lambda}_i}{\Delta x} + k\right) i\right] \dot{W}$$

Results

- To date we are finishing the verification process of this new code.
- Two separate test cases have been choosen

  One-dimensional unsteady channel flow
  Laminar vortex shedding from a cylinder

Results (cont.)

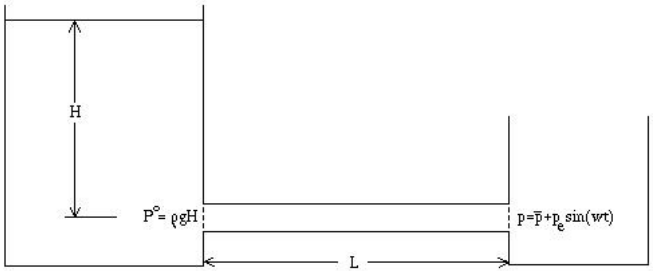

- Merkle and Athavale (1987) have derived an analytic solution based on linearized perturbations for incompressible channel flow. The periodic steady state solution is

$$\acute{u}(t) = -\frac{\acute{p}_e}{\rho \bar{u}} \left(\frac{1}{1+\Omega^2} \right) \left[\sin(wt) - \Omega \cos(wt) \right]$$

$$\acute{p}(x,t) = \acute{p}_e \sin(wt) + (x-L) \frac{\acute{p}_e}{L} \left(\frac{\Omega}{1+\Omega^2} \right) \left[\Omega \sin(wt) + \cos(wt) \right].$$

Results

- Channel flow boundary conditions

Exit pressure perturbation	$\frac{\acute{p}_e}{\bar{p}}$	1e-4
Reduced frequency	$\Omega = \frac{wL}{\bar{u}}$	1.0
Mean flow mach number	$\bar{M}$	0.1
Constant inlet stagnation pressure		

- A single frequency is excited at the exit.

- 17 grid points are used along the length of the duct.

Results (cont.)

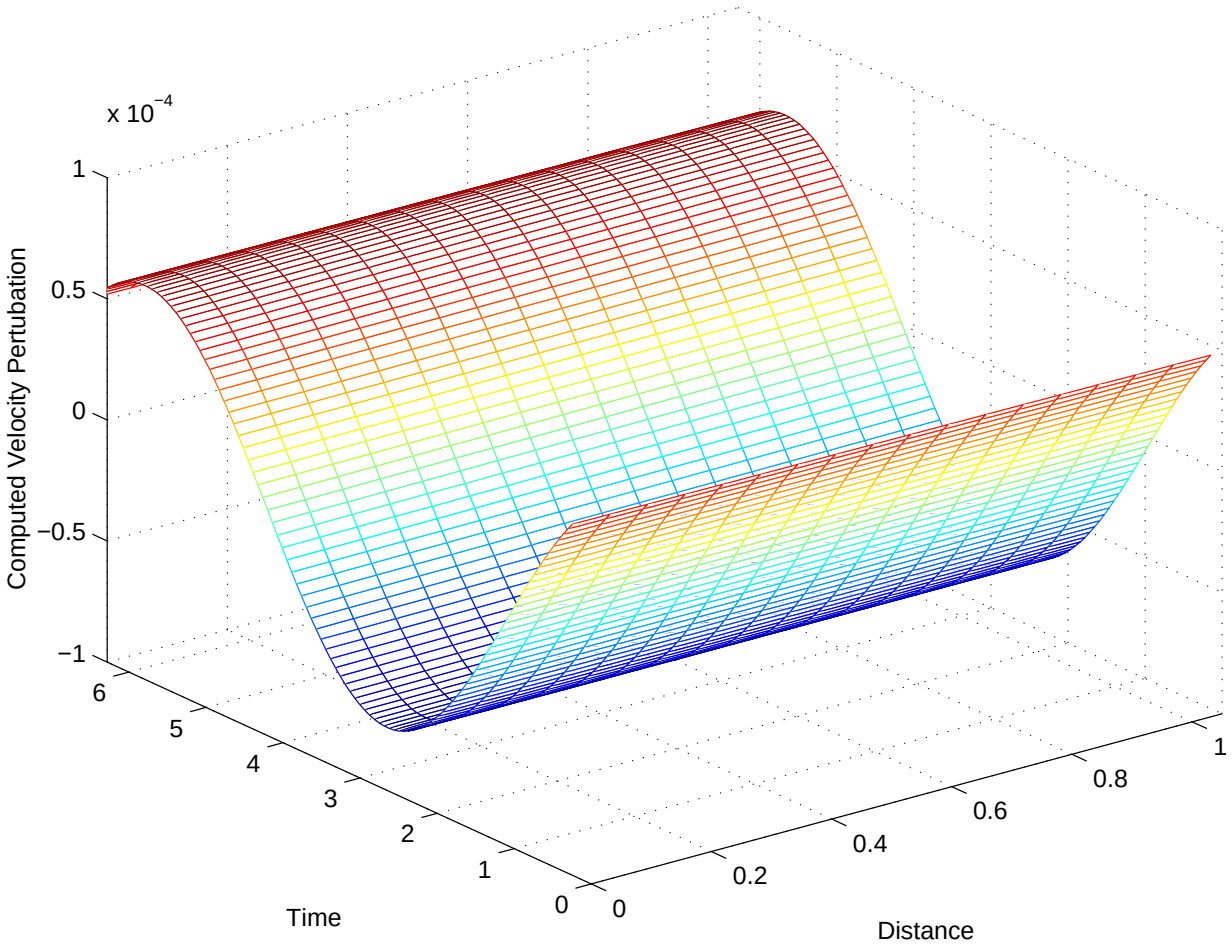

Results (cont.)

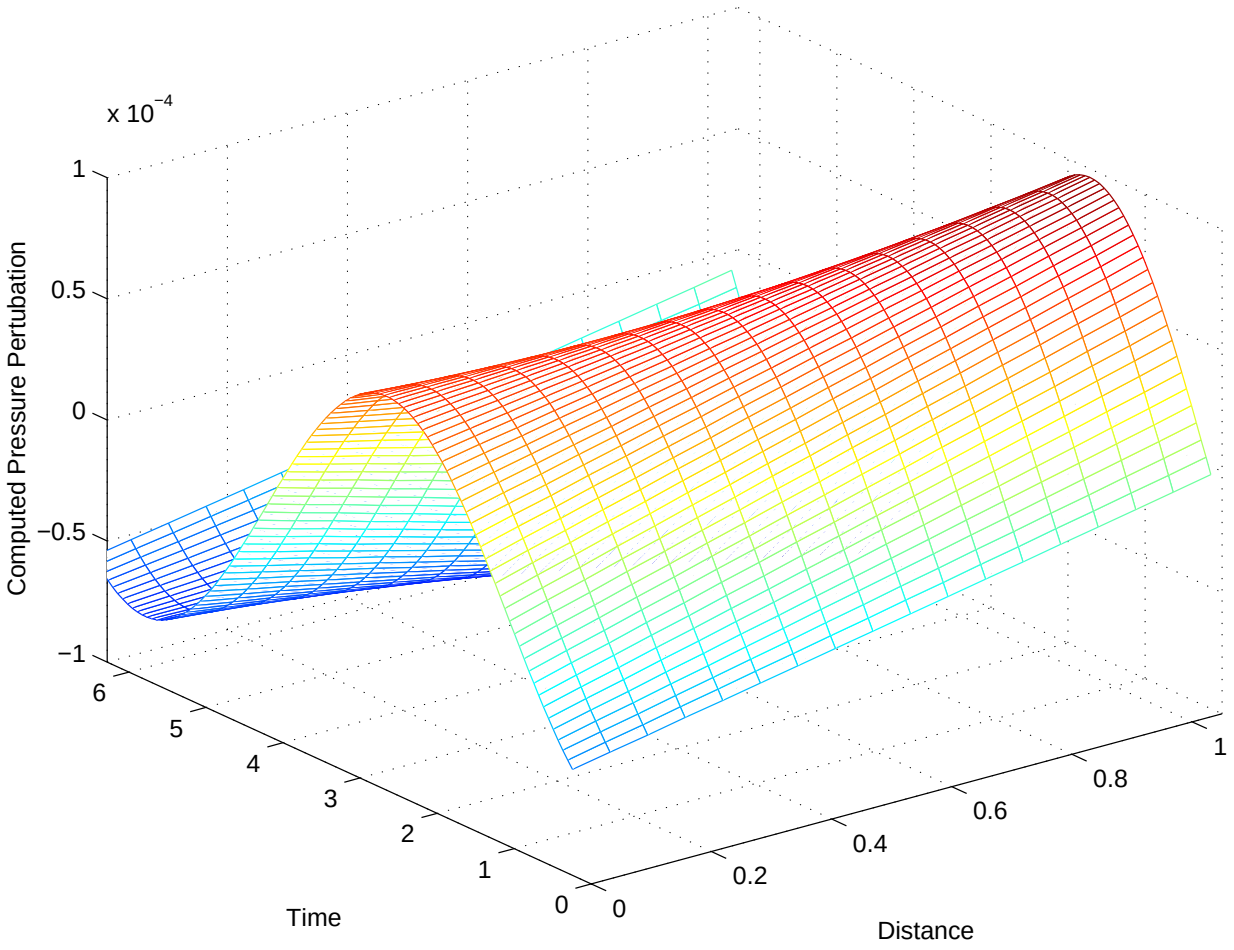

Results (cont.)

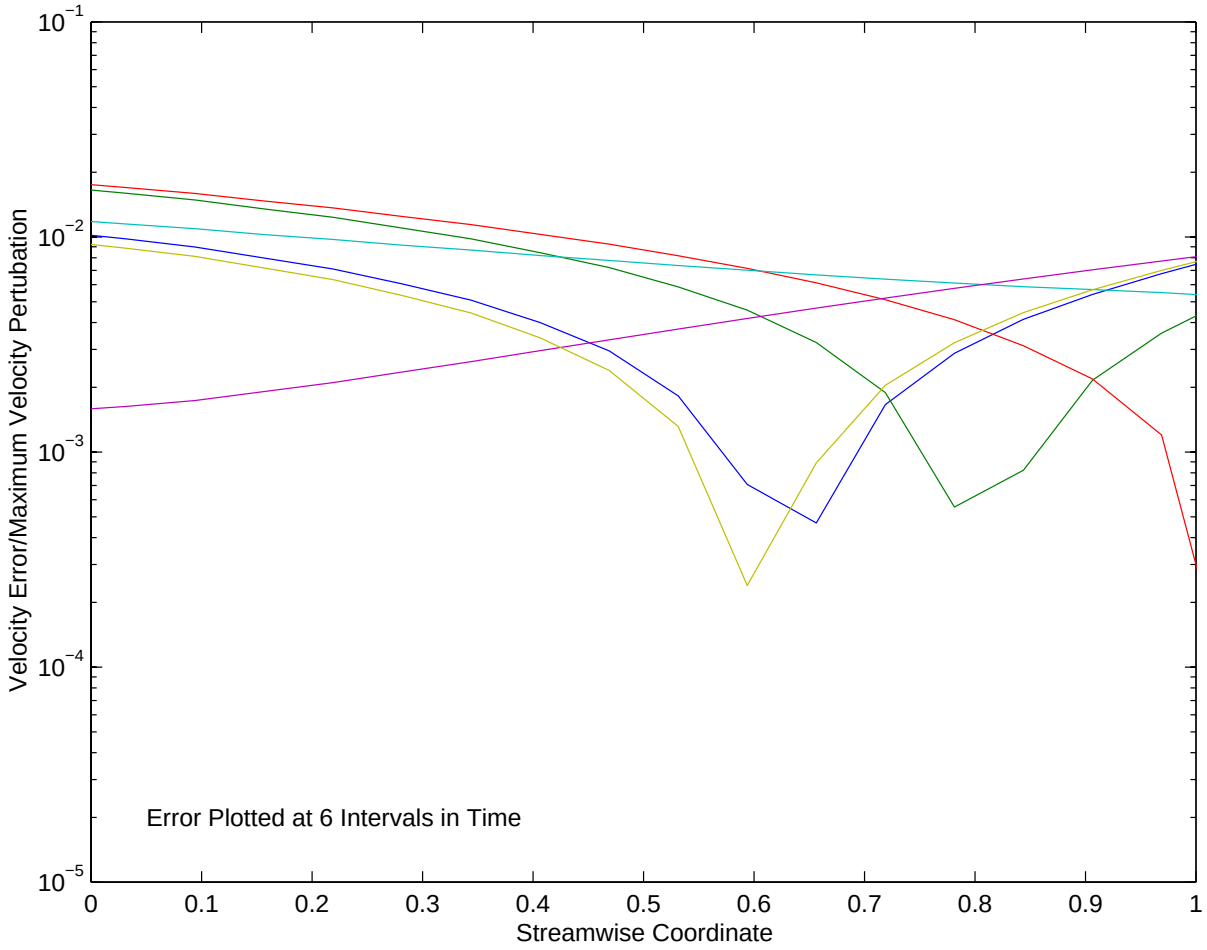

Results (cont.)

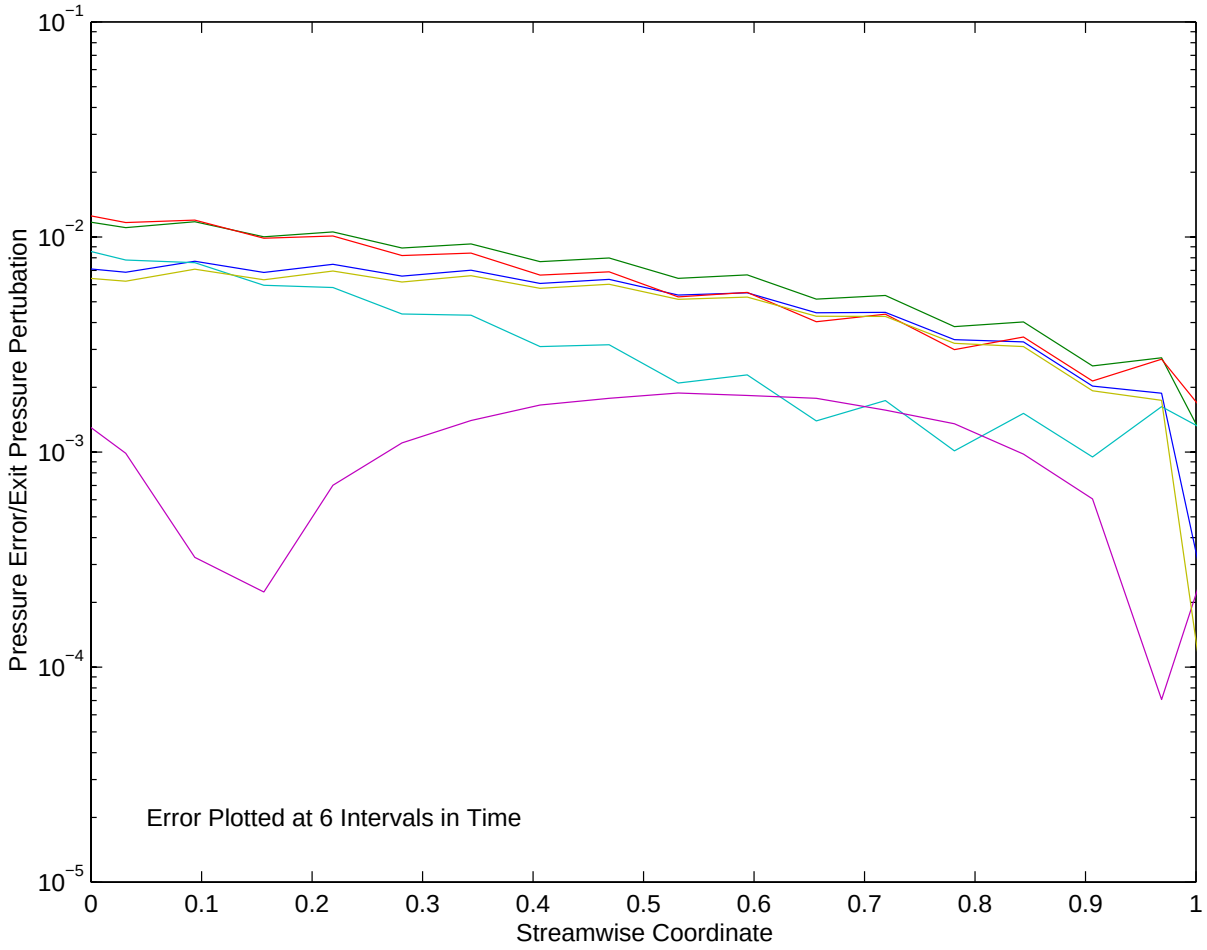

Results (cont.)

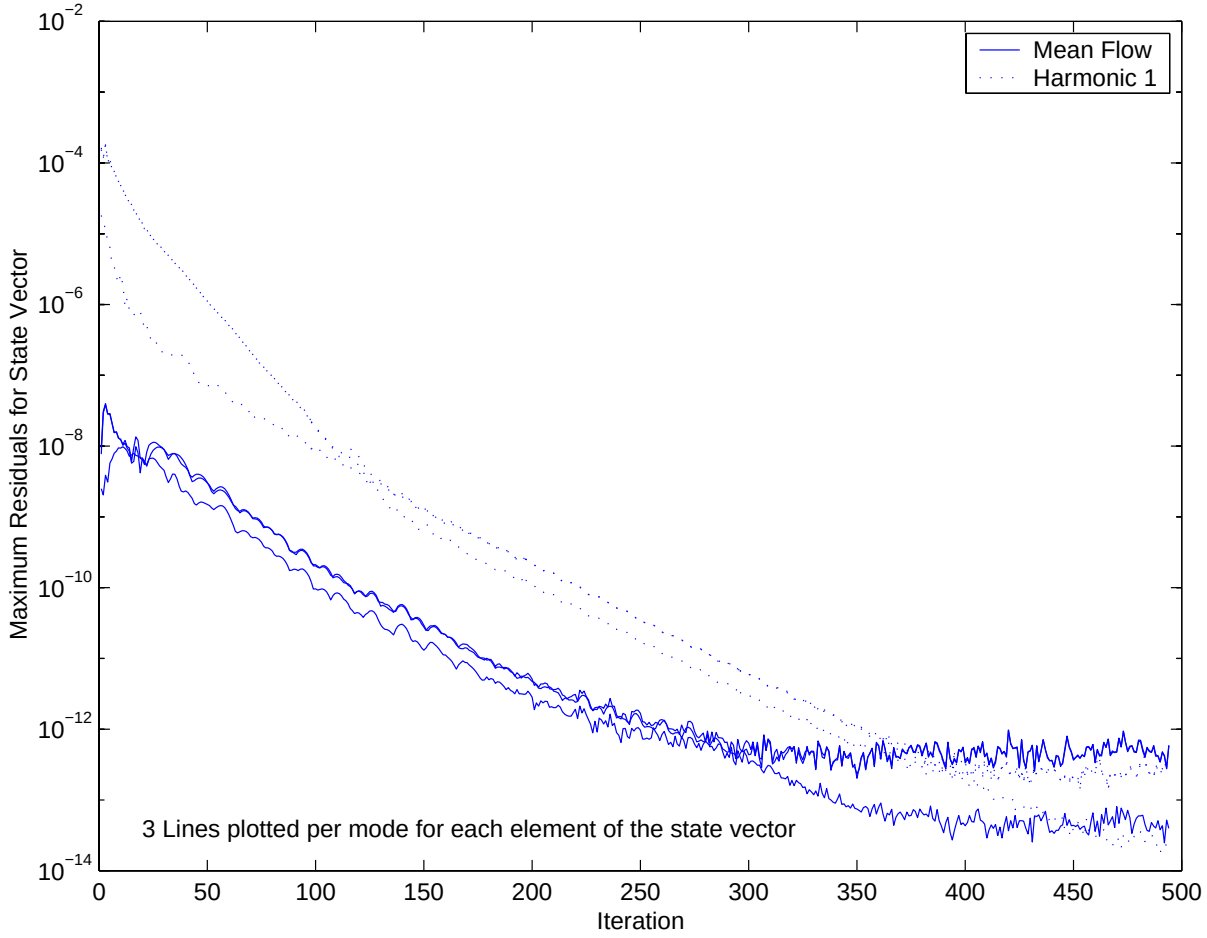

Results (cont.)

- The solution in the channel flow test case contains unsteady perturbations small enough to be modeled using linear theory. We choose our second test case as cylinder flow at a Reynolds number of 180. The non-linear capabilities of the harmonic balance solver are tested by the unsteady perturbations associated with the Karman vortex street.

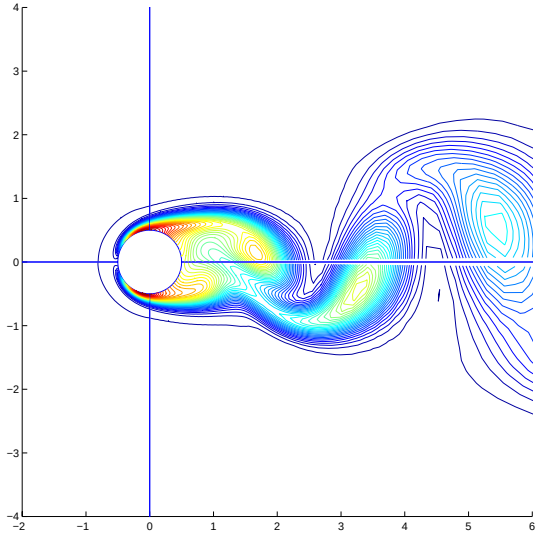

Results (cont.)

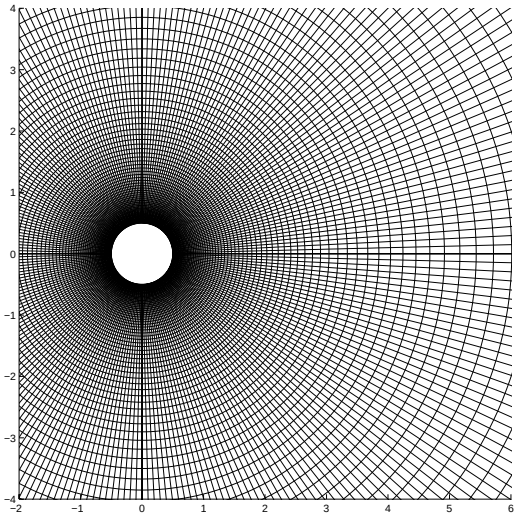

- The grid size is 256 by 128 cells. The mesh boundary is 200 chords from the center of the cylinder. An exponential stretching function is used in the radial direction with the smallest grid spacing of $3.54e-03$ chords occurring at the wall. At the top of the cylinder roughly 15 grid points captured the boundary layer.

Results (cont.)

Experiment	$-C_{pb}$	C_d	S_t
Williamson and Roshko (1990)	0.83		
Roshko (1954)			0.185
Wieselsberger (1922)		1.3	
Henderson (1995)	0.83	1.34	

Table 1: Time Averaged Experimental Data

Temporal Modes	$-C_{pb}$	C_d
1	0.832	1.257
3	0.895	1.306
5	0.903	1.311
7	0.903	1.311

Table 2: Time Averaged Data versus Temporal Modes

Results (cont.)

- Contours of the X Component of Velocity - 7 Temporal Modes

Time=0

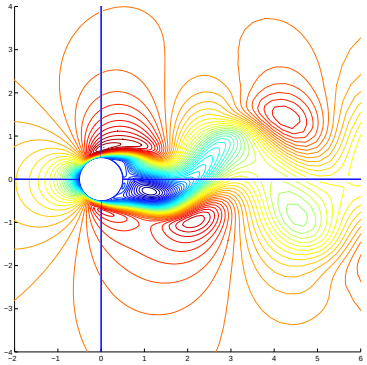

Time=$\frac{\tau}{4}$

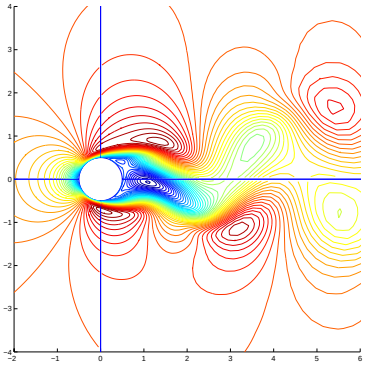

Time=$\frac{\tau}{2}$

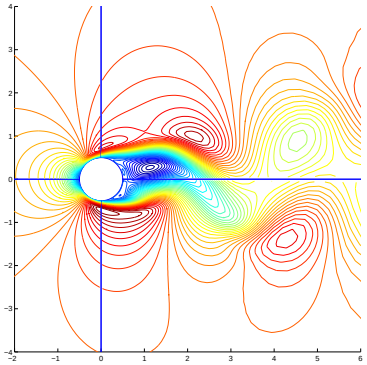

Time=$\frac{3\tau}{4}$

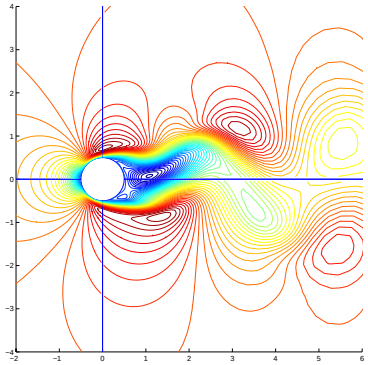

Results (cont.)

- Contours of the Y Component of Velocity - 7 Temporal Modes

Time=0

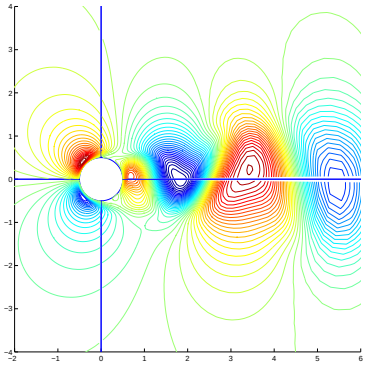

Time=$\frac{\tau}{4}$

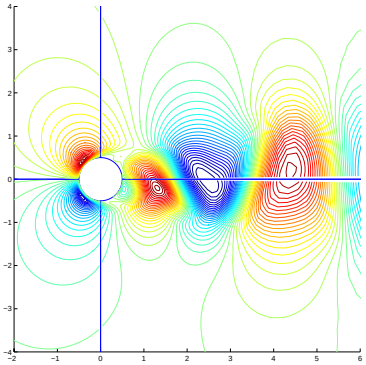

Time=$\frac{\tau}{2}$

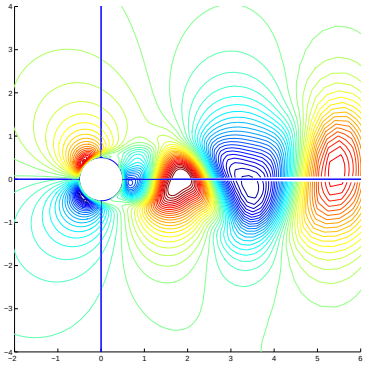

Time=$\frac{3\tau}{4}$

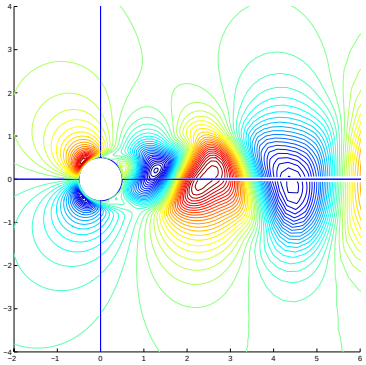

Results (cont.)

- Contours of Pressure - 7 Temporal Modes

Time=0

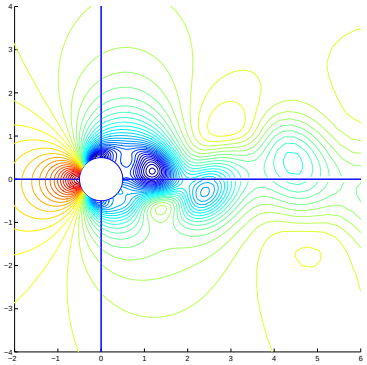

Time=$\frac{\tau}{4}$

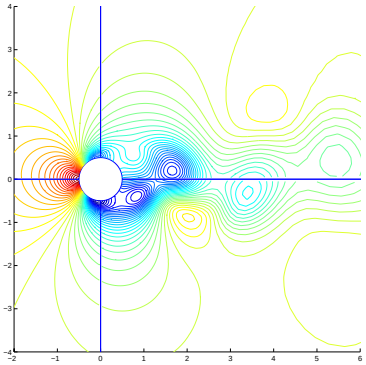

Time=$\frac{\tau}{2}$

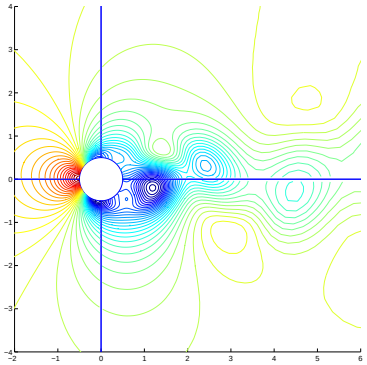

Time=$\frac{3\tau}{4}$

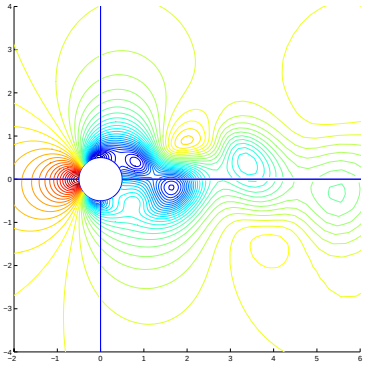

Results (cont.)

- Contours of Entropy - 7 Temporal Modes

Time=0

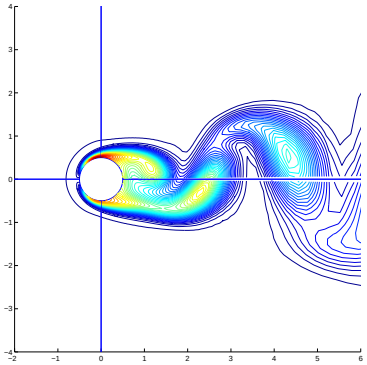

Time=$\frac{\tau}{4}$

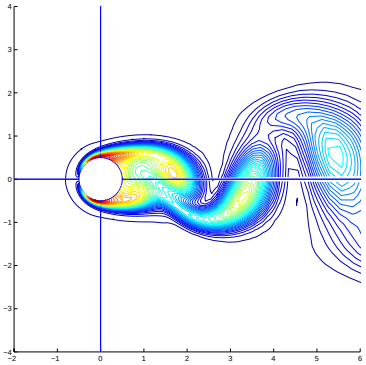

Time=$\frac{\tau}{2}$

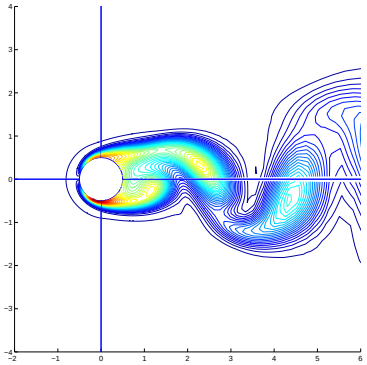

Time=$\frac{3\tau}{4}$

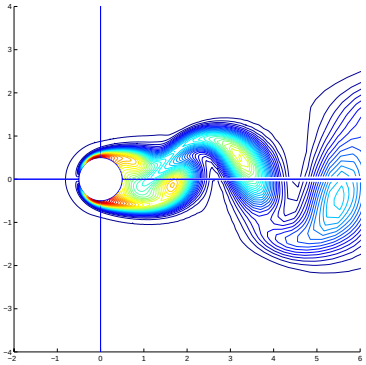

Conclusions

- An unsteady solver for the fully non-linear viscous Navier-Stokes equations has been developed. Harmonic balance techniques are used to transform the unsteady equations in the physical domain into a steady system in the frequency domain.

- To verify the code, numerical experiments were performed on an unsteady channel and a cylinder shedding periodic vortices.

- The results showed good agreement with the analytic and experimental solutions.

Conclusions (cont.)

- A limited number of temporal modes could accurately resolve time averaged flow field quantities.

- We believe that it could be very beneficial to use the harmonic balance method to provide an initial solution for fully time accurate unsteady simulations. This should eliminate the need to integrate the solution over a large number of periods before reaching a periodic steady state.

Future Work

- Continue verification process to turbomachinery cases where experimental data exists.
- Modify TFLO code to implement harmonic balance techniques.
- Perform side-by-side comparisons between dual time stepping and harmonic balance methods.